JOURNAL OF SPACECRAFT AND ROCKETS
Vol. 31, No. 6, November–December 1994

Imaging Penetrator-Beacon Design for Mars

Dan G. Tuckness*
University of Texas at Arlington, Arlington, Texas 76019-0018

A navigation sensor design using penetrator beacons to support a precision Mars surface-relative navigation scenario is presented. Penetrator beacons are small ballistic vehicles that would precede a soft lander to image a proposed landing region and establish a network of surface-relative radio navigation beacons. It is proposed that the use of penetrator beacons could support a precision landing, could meet mission navigation accuracy requirements, would not require additional mission elements such as an imaging orbiter, and could be designed using current technology, thereby reducing costs. Investigations concluded that penetrator beacons could provide high-resolution images of a landing region and provided a network of radio navigation beacons within the proposed landing region.

Introduction

FUTURE Mars exploration missions, both robotic and piloted, may have stringent navigation accuracy requirements. One of the most stringent of these requirements is to land a spacecraft autonomously in a very small area (approximately 10 m in diameter) that is clear of all surface hazards.[1] The safety and survivability of these landing vehicles will depend on first selecting safe landing sites, precisely targeting the lander to specific points on the surface, and performing terminal guidance to land at these points.[2–4]

The Mars Rover Sample Return (MRSR) is used as a reference mission for this investigation, but it is understood that the penetrator-beacon navigation method can be used for any mission requiring surface relative navigation. The MRSR landing spacecraft (lander) will be required to land in an area that is scientifically interesting. Unfortunately, many of these geologically interesting regions on Mars have few safe landing sites (free of surface hazards). Rocks with diameters less than 1 m and surface slopes less than 15 deg over a 10-m baseline are mission requirements of the MRSR mission and are generally considered mission requirements for a lander's tolerance of surface hazards.[2–5] This presents several navigation problems:

1) The navigation system must be sophisticated enough to find a touchdown point within an area of hazardous terrain that will provide a safe landing.

2) Information about the surface characteristics of Mars is limited to previous lander imagery, previous and current orbiter imagery (Viking Orbiters), thermal imagery, and radar roughness data. The Viking Orbiter spacecraft has imaged the surface of Mars with a resolution of 200 m/pixel or better, with approximately 0.03% of the surface imaged to a resolution of approximately 10 m/pixel. However, to observe 1-m obstacles and surface slopes less than 15 deg over a 10-m baseline, resolution on the order of 0.25 m/pixel must be obtained.[1]

3) Earth-based radiometric tracking of the lander while in Mars orbit provides a very precise determination of the spacecraft orbit about Mars. However, those measurements are relative to the Earth inertial frame and not the Mars inertial frame. The difference between the two inertial coordinate frames (sometimes called inertial-map error or frame tie error) for the MRSR mission is estimated to be 100 m (1σ), which is orders of magnitude greater than the size of the predicted certified landing sites (10 m).[1] This results in the descent and landing trajectory incorporating the inertial-map error, which in turn results in a terminal landing position error of no less than the inertial-map, error. Therefore, landing in a certified site within 10 m of a surface feature will require surface-relative navigation capabilities.

There are many solutions to the safe-landing problem, but generally they can be broken into two philosophies: active hazard avoidance or precision landing.

1) The active hazard avoidance approach would enable the vehicle to locate, identify, and avoid hazards that threaten the success of the landing. Imaging systems that provide rapid high-resolution images to the Lander's computer would have to be developed, algorithms for the identification of obstacles and hazards would have to be perfected, and finally an expert system capable of interrogating the images and commanding the vehicle in real time would have to be synthesized.

2) The precision landing approach would find a suitable landing site prior to deorbiting the spacecraft and then would navigate the landing vehicle to the preselected site. Present thinking would select the landing site on the basis of imagery acquired from an imaging orbiter.[6] This would relieve the high cost of developing and constructing a hazard avoidance system. As a consequence of reducing cost of the lander navigation sensor suite, however, additional mission cost would accumulate in the form of mapping and processing large amounts of Mars imagery along the descent, entry, and landing trajectory to remove inertial-map error and relative-map error. The latter is the error introduced when two images of a planetary body are used for surface relative navigation for one common trajectory and they do not contain the same surface features (images or maps do not overlap).

Similar to the precision-landing scene-matching method, the penetrator-beacon navigation method uses surface features to remove the inertial-map error.[7] It also uses overlapping images to remove the relative map error. This approach would use the penetrators' onboard camera to photograph the landing-area terrain during descent, send this image information back to Earth via an orbiting lander relay, and allow Earth-based ground controllers to select a suitable landing site within the images. This information is sent back to the lander in the form of distance and bearing from the radio frequency (rf) beacons mounted on the penetrators to the selected landing site.

This investigation discusses the possibility of a penetrator-beacon method and presents a preliminary mission/system design. The basic structural design of the penetrator-beacon vehicle is a derivative of the penetrator design found in Manning.[8]

Overview of the Penetrator-Beacon Scenario

The penetrator-beacon scenario begins after the landing spacecraft has established orbit around Mars. Before separation, the penetrator cluster containing the penetrators will be attached to the lander spacecraft via the penetrator terminal deaccelerator shell. Figure 1 shows the penetrator cluster and aeroshell in the entry configuration. Power management will be supplied to the penetrator

Received Jan. 23, 1993; revision received April 2, 1993; accepted for publication April 5, 1993.

*Assistant Professor, Department of Mechanical and Aerospace Engineering, Box 18018. Member AIAA.

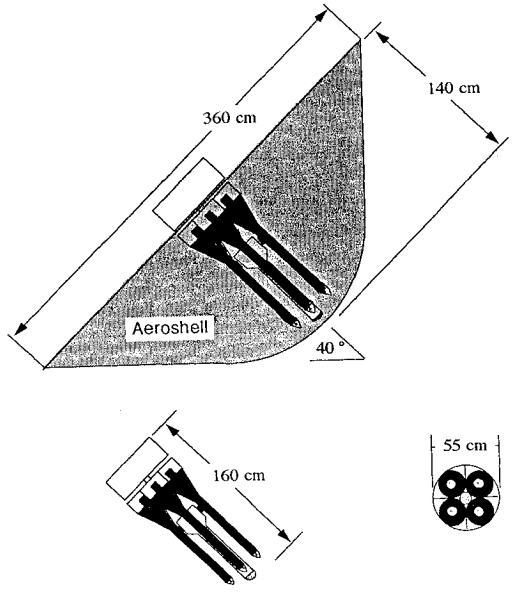

Fig. 1 Penetrator cluster and aeroshell.

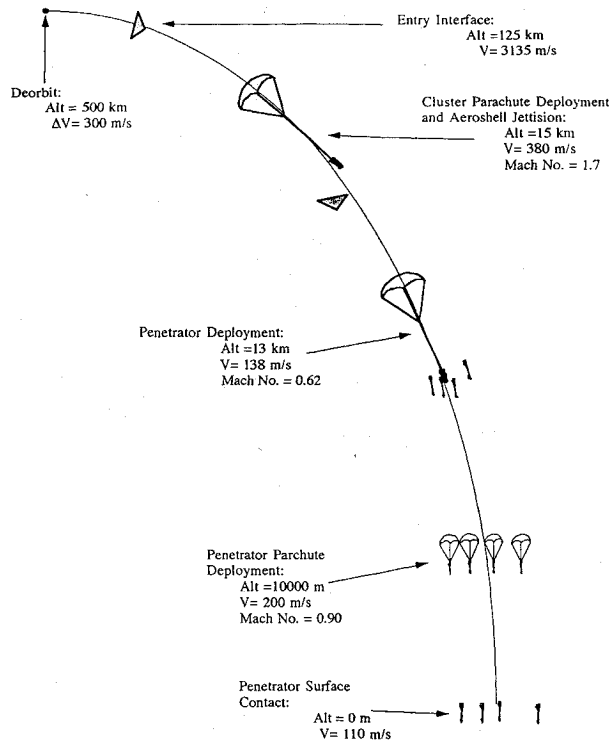

Fig. 2 Scout beacon scenario.

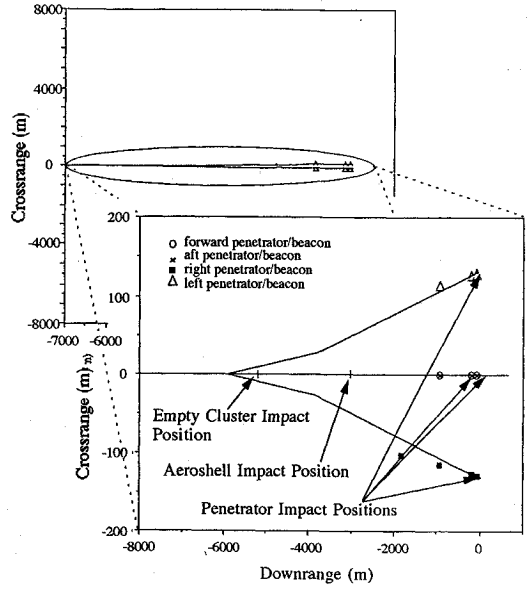

Fig. 3 Penetrator terminal groundtrack and impact point.

from the lander for housekeeping purposes, and the lander will relay engineering data to Earth as part of its nominal data stream. The separation maneuver is divided into two parts: pointing by the lander and propulsion by the penetrator cluster. The actual position of the landing site for each of the penetrators is determined primarily by the lander's orbit and the accuracy of the separation maneuver, aerodynamic errors, map/pole errors, and winds. Studies have shown that downrange dispersions associated with the deployment of the penetrator-cluster aeroshell can vary up to 40–50 km (3σ), with crossrange dispersions up to 15 km (3σ) depending on the initial deployment conditions.[9] The Viking mission had dispersion errors of 70 km downrange and 50 km cross range (3σ).[10] However, selecting the penetrator impact target area ("safe" landing area) a priori, based on the dispersions, will result in a penetrator surface impact within an area containing no hazards that violate MRSR mission requirements. Adopting the dispersion errors found by Swenson as an approximate dispersion for this penetrator-beacon design, images of the surface obtained by the Viking landers will be analyzed to select and certify the 50 × 15-km safe landing area on the surface. The safe landing area will be defined as a surface area (or region) that will contain a hazard frequency distribution that certifies, with a probability of confidence that meets mission success requirements, the existence of 10-m landing areas containing no hazards with diameters greater than 1 m and surface slopes less than 15 deg over a 10-m baseline. This is the same basic approach used to select the Viking presumed-lack-of-hazards landing sites.[11]

The cluster aeroshell will be deployed from the lander spacecraft, will initialize its attitude, and then will fire its spin thrusters to start the vehicle spinning in order to spin-stabilize it for the deorbit maneuver. The design of the cluster aeroshell and its spin stabilization should be such that an active attitude control system will not be required. The cluster aeroshell will then conduct a deorbit burn that sends it toward entry interface (defined as 125-km above ground level). The inertial-flight-path angle at entry interface should be at least 10 deg to avoid skipout, but shallow enough to assure acceptable heat loads on the decelerator. A flight-path angle of 10 deg was selected to minimize the deorbit ΔV. Following the deorbit burn, the cluster aeroshell will fire its despin motors to reduce the spin rate for entry into the atmosphere. The cluster aeroshell proceeds through the atmosphere, and at 15 km above the surface of Mars a parachute is deployed to decelerate the penetrator cluster and to separate it from the aeroshell. At 13-km altitude, the penetrator deployment springs will simultaneously eject the penetrators out and away from the penetrator mounting cluster, and the penetrators will deploy their individual parachutes. Finally, at 10,000 m above the surface, the penetrator parachutes will be jettisoned and the penetrators will be allowed to free-fall to the surface, resulting in an impact velocity of approximately 110 m/s. Figure 2 illustrates the penetrator-beacon scenario.

The penetrators will be mounted 90 deg apart on the penetrator mounting cluster and will thus have an initial relative motion 90 deg away from each other upon deployment. The four penetrators will be ejected simultaneously and should trim out 2–3 s after ejection. This relative motion will continue until impact, and because their initial downrange velocity component is large compared to the ejection velocity, all of the penetrators will impact the surface in a cluster formation downrange of their deployment point. Figure 3 shows a planform view of a typical trajectory of a set of four penetrators and the center location of the penetrators' field of view (FOV). Penetrator trajectory and surface relative flight path angles are shown in Fig. 4.

Each penetrator will be carrying an imaging system in its nose, as shown in Fig. 5. Approximately 30 s after ejection from the penetrator mounting cluster, the penetrators will begin to image the

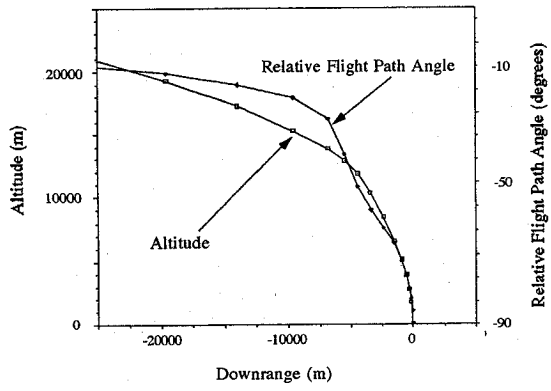

Fig. 4 Penetrator altitude and flight-path angle vs altitude.

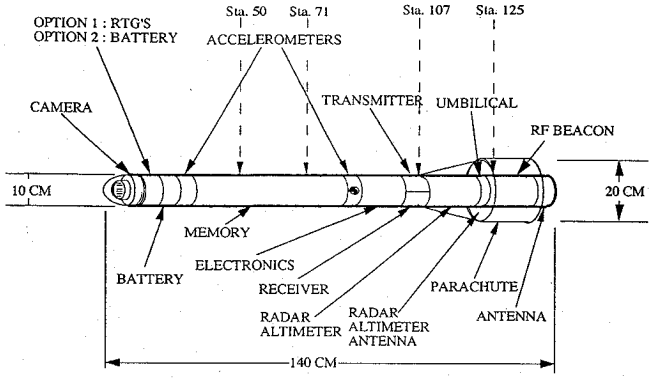

Fig. 5 Penetrator beacon.

surface below them. Because the penetrators are fairly close together (less than 250 m apart) and their FOVs are large, the penetrators will image common overlapping areas. Each penetrator will acquire four images of the surface within altitudes ranging from 2 km to 100 m above the surface. The total area imaged by all four penetrators will vary from about 1.5 km^2 for the first image at a resolution of approximately 0.7 m/pixel to 1607.05 m^2 for the last image at a resolution of 0.05 m/pixel. The last penetrator image will be at 100 m and will cover a circular area on the surface of Mars with a radius of approximately 20 m. Fixing the impact position of the penetrators within the last image (20-m radius) is currently under investigation. See Ref. 7 for a detailed discussion of the imaging requirements and performance during of the charge-coupled device (CCD) during penetrator descent.

The penetrators will impact the surface of Mars within the imaged area, and, through analysis and trajectory reconstruction using the stored accelerometer and radar-altimeter data, the location of the penetrators relative to the imaged landing sites will be well known. Each penetrator will carry a communication system (beacon) capable of supplying rf ranging to a landing vehicle. The penetrator will store all measurement data onboard its mass storage and transmit the stored data to the Lander in orbit at a later time.

Analysis of Penetrator Descent and Surface Impact

Deorbit, Penetrator Ejection, Descent Trajectory, and Landing Spread

The accessible latitudes of the lander and penetrators will be dependent on the Mars arrival asymptote from its interplanetary transfer. The initial conditions of this study assume the coupled lander-penetrator vehicle is in a 500-km circular orbit. An orbit that results in the lander crossing directly overhead offers the greatest amount of time for line-of-sight data transmission between the lander and the penetrator on the surface. The longitude can be varied from 0 to 360 deg by controlling the hour of arrival. Investigations of the Mars arrival and the orbit inclinations have been deferred for future studies.

The entry design configuration includes two decelerator stages. The first stage (hypersonic decelerator stage) incorporates initial entry deceleration and heating, and must therefore be designed to withstand significant structural and thermal loads. The hypersonic

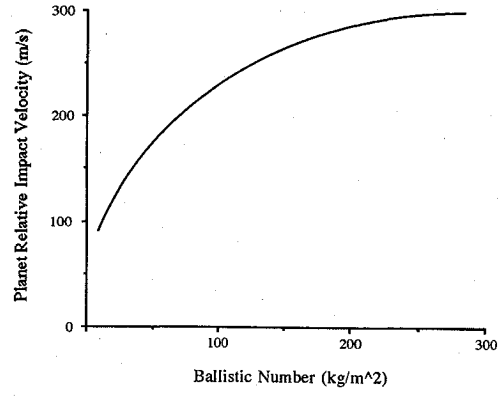

Fig. 6 Ballistic number vs planet relative impact velocity.

decelerator is a 40-deg half-cone, blunt nose aeroshell that covers the four penetrators and the penetrator mounting cluster down to 15 km, where the penetrators are deployed and the aeroshell is jettisoned. The aeroshell uses ablative material to cover the penetrators and penetrator mounting cluster for heat protection. The blunt-nose aids in avoiding excessive heating and asymmetric ablation. It will also result in the aeroshell entering the atmosphere with an angle of attack of approximately 0 deg. This will aid in reducing atmospheric trajectory dispersions.

The aeroshell parachute will be deployed at Mach 1.7, a speed at which the deployment of ordinance may need careful investigation. The primary concern is in the deployment mechanics, the inflation and stability of the canopy (especially for a reefed system), and the aeroheating of the parachute materials for parachutes operating at supersonic speeds. Supersonic parachute deployment results from a performance tradeoff that attempts to keep the aeroshell size and weight to a minimum. This requirement increases the entry velocity of the aeroshell, thereby increasing the parachute deployment velocity. Carter and Smith pointed out a number of new designs (including high-speed drogues and parasonic ballutes) during their investigation into parachute design for the MRSR lander, in which parachute deployment at Mach numbers of 2 and greater were considered.[4] Also, for comparison, the Viking parachutes were designed for deployment at Mach numbers less than 2.1 and were actually deployed at Mach 1.1.[12]

The baseline parachute type selected for this design is a disk-gap-band (DGB) parachute developed by the Planetary Entry Parachute Program (PEPP).[13] A DGB parachute was selected because of its high-Mach-number stability combined with good drag performance. The parachute selected for the aeroshell has a radius of 4.75 m and C_d of 0.65.

A parachute decelerator will be used during the second deceleration stage to insure that the penetrators' flight path angle at impact is as steep as possible, on the order of 80–90 deg. It will also help to reduce surface impact forces (addressed later). The steep flight-path angle is required for the penetrator to properly penetrate the surface of Mars and provide accurate radar altimeter and image information. Each penetrator parachute has a diameter of approximately 2.0 m and is deployed at an altitude of 10.0 km above the surface at subsonic speeds. The penetrators will experience a high deceleration load because of the high velocity at the time of parachute deployment. This load should be much less than that experienced upon impact with the planet surface. It was determined that a parachute decelerator that provides the penetrators with a ballistic number of approximately 15.5 kg/m^2 will slow them to about 110 m/s and result in a flight-path angle of 88 deg (below horizontal) at impact. Figures 6 and 7 show the ballistic number vs planet-relative impact velocity and vs planet-relative flight-path angle, respectively. Basic characteristics of the decelerators are given in Table 1.

At entry interface the aeroshell vehicle will be spinning at approximately 15 rpm and will enter the atmosphere with a 10-deg flight-path angle at a velocity of approximately 3100 m/s. The rotation of the aeroshell is necessary for stability, but it makes the determination of the surface-related ejection direction of the penetrators difficult to determine. Since the position of the penetrator

Table 1 Aerodynamic decelerators

Hypersonic decelerator with penetrator cluster and four penetrators (entry configuration)	
Half cone angle, blunt nose	40 deg
M/CDA	37.0 kg/m^2
Mass	451.0 kg
Penetrator cluster and four penetrators (separated from aeroshell, cluster parachute deployed)	
M/CDA	7.55 kg/m^2
Mass	348.0 kg
Hypersonic decelerator aeroshell only	
M/CDA	8.35 kg/m^2
Mass	102.0 kg
Penetrator parachute decelerator and penetrator	
M/CDA	15.5 kg/m^2
Mass	61.8 kg
Penetrator without parachute decelerator	
M/CDA	> 1500.0 kg/m^2
Mass	51.8 kg

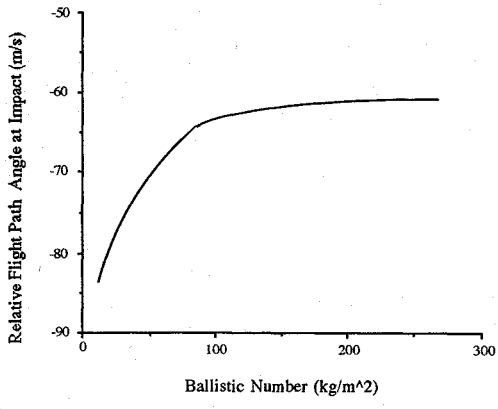

Fig. 7 Ballistic number vs planet relative flight-path angle.

mounting cluster at the time of penetrator ejection will be reconstructed and the orientation of the sun with respect to Mars will be fairly well known, the orientation of the shadows within the images (obtained by the penetrators during their descent) can be used to determine the orientation of the penetrators' images.

The penetrators, when ejected, will have an initial relative motion of 90 deg away from each other. This relative motion should continue throughout the penetrators' trajectory regardless of the spin orientation of the penetrator mounting cluster at the time of ejection. The orientation of the penetrator mounting cluster at the time of ejection will simply serve to rotate the common center of all four images (all four penetrators combined), and the size of the common FOV will be dictated by the altitude of the penetrators. The total velocity of each penetrator is dominated by the downrange velocity of the penetrator mounting cluster at the time of ejection; therefore, regardless of the surface-relative ejection direction, all four will impact in a cluster downrange of the point of ejection.

Because of the limited size of the penetrator mounting cluster and its inability to carry a large deployment device, a deployment velocity of 8 m/s was selected on the basis of providing an average penetrator displacement from centerline of approximately 140 m upon impact. Further, it was assumed that this velocity increment should be achievable with existing hardware.

The penetrators' impact spread should not be affected by the Martian winds, because they are clustered together during initial entry and their ballistic numbers after cluster separation and before parachute deployment are approximately 1500 kg/m^2, which makes them fairly impervious to atmospheric dispersions. However, a thick wind layer at Mars can be assumed to translate the penetrators parallel to the surface while they maintain local vertical orientations. With this conservative assumption, the angle of attack at surface impact is a function of the impact speed and the wind speed. It has been shown that these impact conditions can be related to the depth of penetration and the g load on the forebody of the penetrator for a given soil classification.[14]

The winds affect the penetrators after their parachutes are deployed, because their ballistic number changes from 1500 to about 15.5 kg/m^2. Because all of the penetrators will deploy their parachutes simultaneously and the penetrators are generally less than 150 m apart, the local winds should affect all of the penetrators uniformly. Manning found no actual angle-of-attack test data directly related to penetrators.[8] However, data that do exist (small size and very high impact speeds into reinforced concrete) indicate that for baseline impact speeds (100–160 m/s) a wind of about 14 m/s could be tolerated. A penetrator designed to survive greater g loads at impact would allow larger impact and crosswind velocities. This directly influences the maximum allowable impact angle (angle of attack and side slip angles). Data taken by the Viking spacecraft indicate[15] winds on the order of 10–15 m/s with gusts to about 20 m/s. Since the penetrator pitching frequency should be low, the penetrator will only experience a couple of pitching motion cycles during the last couple of kilometers of the descent. This should be sufficient for the penetrator orientation to adjust to terminal wind conditions before impact.

Surface Impact

Terrain impact testing of a penetrator has shown acceptable penetration in 25% porous basalt and in moist loess.[8] According to Ref. 8, slopes up to 45 and 60% are expected to yield successful-penetration probabilities of nearly 100 and 50%, respectively. Other tests have also been performed to study penetrator impact. To test the feasibility of the concept of a lunar penetrator, Mizutani and Kawashima[16] have conducted experiments on the impact of penetrator models onto an analog of lunar soil, using a single-stage gas gun in a vacuum chamber. Their penetrator design was experimentally proven to withstand an impact of 300 m/s. Also, success of penetration into sufficiently smooth and homogeneous soil can be estimated from field test data. Field drop tests have been demonstrated where penetrators can survive emplacement in solid basalt formations.[8]

An important area of concern is whether a penetrator will survive impact with rocks of size such as that found in the Viking I and Viking II photographs. Manning investigated the probability of penetrator failure due to impact with surface rocks and concluded that surface rocks observed at the Viking landing sites do not appear to be an undue threat to the stability of the impacting penetrator. In their report it was stated that they investigated only the distribution of surface rocks. It was also stated that rocks embedded in the soil at shallow depths might also cause deflection in the path of the penetrator. However, their field test indicated that soil already penetrated had a stabilizing effect when the penetrator struck a subsurface rock structure.

Penetrator System and Subsystem Design

Penetrator Structure

The penetrator is rocket-shaped; it has a blunted ogive nose containing the descent camera and a conical flared aft section with a tapered sidewall thickness. Figure 5 shows the penetrator beacon and its various systems. After impact the afterbody (containing the rf transmitter) remains at the surface. The penetration depth of the forebody is influenced by the weight/(frontal area), impact-site velocity and material properties, and angle of attack.

The structure of the Mars penetrator should withstand impact loads of 1800 to 2000 Earth g, and be able to penetrate a wide range of soil densities from 1 to 15 m. The Manning design features a forebody outer casing constructed using HY 180 steel and an afterbody made from 7075-T7351 aluminum. The avionics assembly structure is machined from 7075-T7351 aluminum. A tangent ogive nose with a length-to-diameter ratio (L/D) of 2.4 was chosen because of its proven performance characteristics. Because the descent imaging camera will be contained in the nose, investigations into using a hardened transparent medium that can retain most of its shape

Table 2 Mass, power, and volume estimates for one penetrator

	Weight, kg	Volume, cm^3	Power, mW	
			Standby	Peak
Penetrator subsystems				
RTG (Li-BCX batteries optional)	1.40 (1.40)	900 (500)	—	—
Li-BCX batteries	2.00	500	—	—
Power control	0.34	200	—	—
Accelerometers (6)	0.18	180	0	180
Central process unit	1.00	1000	50	1000
Bubble memory, 17 Mbit	4.00	2000	0	5000
Umbilical cable	0.70	700	0	0
Transmitter	0.50	300	0	5000
Receiver	0.50	360	100	200
Antenna	0.50	500	0	0
Rf navigation beacon	5.00	800	0	9000
Radar altimeter	4.00	820	0	10000
Imaging camera	2.00	500	300	4000
Heat pipe	0.30	430	0	0
Parachute	10.00	1700	0	0
Structure	30.00	—	0	0
Total	62.42 (62.42)	10890 (10490)	450	34380
Cluster and aeroshell				
Aeroshell structure and ablator	102.00			
Penetrator cluster and ejection system	50.00			
Parachute and parachute mortar	45.00			
Deorbit engine	3.00			
Tanks and structure	1.00			
Spin system	1.00			
Deorbit fuel	2.00			
Total	204.00			
System mass total				
Carrier vehicle	204.00			
Penetrators (4)	249.68			
Total	453.68			

during impact for proper penetration will be required. The length and diameter of the penetrator were chosen to provide stability and bending resistance during penetration. The diameter is a constant 10 cm to station 50. The diameter increases as a cone to 11-cm diameter at station 71, which is maintained to station 107, where it again increases as a cone to a radius of 20 cm to station 125, where the radius remains for the rest of the 140-cm length. This design is based upon a proven concept which has a ratio of weight to cross-sectional area equal to $(W/A)_{CS} = 16.27$ N/cm^2 for the thick-wall section and 20.0 N/cm^2 for the thin-wall section, and L/D of approximately 13.0. Manning's test results show that the penetrators survived penetration of 30 cm of reinforced concrete.[8]

Penetrator Mass, Power, and Volume

The penetrator, as shown in Fig. 5, will consist of a rigid structure, a CCD camera in the nose, a radar altimeter, two sets of accelerometers (three accelerometers per set), a radioisotope thermal generator (RTG), lithium-bromine (Li-BCX) batteries, memory for data storage, and a communication system capable of supporting rf ranging. Because of the large g loads upon impact (possibly 100g or more), an RTG may be impractical to use. This is because the power conversion element (essentially a set of thermocouples) of the RTG is destroyed during a high-deceleration impact. RTGs have been tested to withstand impacts of up to 40 g and could be hardened to withstand impacts up to 100 g, but it is very unlikely that they can be made to survive 100–2000 g. Therefore, two separate power systems will be addressed in the next subsection. Option 1 uses an RTG–Li-BCX combination for impacts of 40 g or less, and option 2 uses only Li-BCX batteries capable of withstanding g loads up to 2000 g. The penetrator-cluster aeroshell system will require two umbilical connectors with the lander spacecraft: one to power the squibs used during the separation phase, and the other for command and telemetry circuits.

Table 2 summarizes the characteristics of the penetrator subsystem and payload. Mass, power, and volume requirements are delineated. In addition, the mass of the components for the cluster aeroshell is given.

Power Requirements

The low data rate of the penetrator will require the storage of data as they are acquired during the descent, rather than transmission in real time. The penetrators will store image data, altimeter data, and accelerometer data during their descent and will transmit the data back to the orbiting lander after impact on Mars. The penetrators' communication system is designed for a 2500-bit/s transmission bit rate and an 800-bit/s command bit rate. Each image consist of 16 Mbit (compressed) of data. Using a 2500-bits/s transmission rate, it will take an estimated 107 min to transmit all four images per penetrator. Assuming the lander passes directly overhead in its 500-km orbit, it will remain 20 deg above the horizon for approximately 605 s. Assuming only zenith passage of the lander in orbit for preliminary estimates and knowing that the penetrator requires approximately 2 h to transmit its acquired information, the lander will be required to pass overhead approximately 11 times. Zenith passage of the orbiting lander is dependent on the lander orbit and could be achieved if the lander were placed into a 1-sol orbit that arrived at periapsis near the zenith point of the penetrators. However, this would require the lander to deorbit from apoapsis for landing, which could result in large navigation errors due to the lengthy deorbit time. Tradeoffs between the lander orbit and transmit passages are currently under investigation.

The penetrator power profile consists of three parts: 1) a steady low-level power requirement to operate the onboard computer during most of a solar day, 2) high power to operate the bubble memory and the imaging components during descent and data transmission

Table 3 Power budget for penetrator

	Power, mW	Energy, W·h	
		Option1[a]	Option2[b]
	Sources		
Primary power			
RTG @ 4% efficiency, 3.08 W	2000.000	25.000	
Inverter efficiency @ 90%	−200.000		
Battery charge efficiency @ 60%	−800.000		
Total	1000.000	25.000	
Secondary/peak power			
JSC (Li-BCX) Battery,	2000.00	200.00	
JSC (Li-BCX) Battery	2000.00		350.000
Total			350.000
	Descent, 19.18 W peak		
Camera, 4.0 W for 50 s	−1.200	0.054	0.056
Accelerometers, 0.18 W for 1700 s	−3.366	0.083	0.086
Radar alt., 10 W for 720 s	−79.200	1.954	2.000
Image storage, 5 W for 12 s	−0.660	0.016	0.017
Radar alt. storage, 5 W for 720 s	−39.600	0.977	1.000
Accel. data storage, 5 W for 4 s	−0.220	0.005	0.006
Total	−124.246	3.089	3.165
	Data transmit, 10.00 W peak		
Transmitter, 5 W for 107 min	−353.100 av.	8.709	8.920
Image dump, 5 W for 107 min	−353.100	8.709	8.920
Radar alt. data dump, 5 W for 720 s	−39.600	0.977	1.000
Accel. data dump, 5 W for 4 s	−0.220	0.005	0.006
Total	−746.020	18.400	18.846
	Rf ranging, 8.00 W peak		
Rf beacon, 8 W for 10 min	−52.800	1.302	1.330
Total	−52.800	1.302	1.330
	Other, 0.25 W peak		
Receiver, 0.2 W, 10% duty cycle	−20.000 av.	0.493	0.480
Microcomputer, 0.050 continuous	−50.000	1.233	1.200
Total	−70.000	1.726	1.680
	Standby, 0.25 W peak		
Receiver, 0.2 W, 10% duty cycle, 190 Earth days			91.200
Microcomputer, 0.050 W, continuous, 190 Earth days			228.000
Total			319.200
Primary net power gain	6.934	0.483	

[a]RTG–Li-BCX battery combination.
[b]Li-BCX batteries only.

periods, and 3) high power for rf communication to the lander for navigation.

As mentioned earlier, two power systems are addressed. The first design (for impact loads of less than 40 g) consists of a secondary system of lithium batteries to provide the power for the transmitter, the memory, and the rf beacon during peak loads and power backup. An RTG is used to provide low-level power and recharge the secondary battery power system. This design allows the penetrator beacon to remain functional for a longer period of time, since the secondary battery system can be recharged using the RTG. This longer life span will allow Earth-based ground controllers more time to assess the images, obtained by the penetrators during their descent, for the desired landing sites. It might also allow the rf beacons, mounted on the penetrators, to be reused at a later date. The second design, using only Li-BCX batteries (for impact loads of less than 2000 g), reduces the life span of the penetrator-beacon system because there is no alternate power source in the design for recharging the batteries. This design yields a 190-Earth-day penetrator-beacon lifetime. A majority of the power is consumed in the standby mode while the Earth-based ground controllers investigate the surrounding terrain images and decide upon the desired landing site, and the MRSR vehicle positions itself for deorbit and landing. A conceptual power budget for the two designs is given in Table 3.

Communication Requirements

A few minutes before interrogation by the lander is to start, the penetrator timer turns on the command receiver. Likewise, the lander command transmitter is turned on to be prepared for the encounter. When the lander elevation angle is greater than 20 deg (to avoid multipath losses and irregular terrain), the lander addresses the penetrator. As the penetrator detects its address, it turns on its transmitter and acknowledges the address. The lander then commands the penetrator to update its clock timer, to make any changes necessary, and then to read out the stored image data during the period for which a good link is expected. The penetrator transmits until either all the data are transmitted or the commanded link duration is reached. Any

data remaining in memory will be read out next time before any subsequently collected data. Thus, the data will always be transmitted in the order acquired. Because of the small size of the penetrators, they will have very limited space for power generation and storage. Because of the lack of available power, the penetrator communications and beacon system will be required to have a low data rate (on the order of kilobytes per second). After separation, the only interface will be a relay link to and from the penetrator. Commands from the lander will be used to change penetrator operating modes and read out the penetrator memory to the lander.

The lander could be designed to have multiple receivers to support simultaneous transmission from the closely arrayed ground stations (penetrators). This would require multiple telemetry carrier channel frequencies, but would reduce the number of lander orbits for reception of image data. Furthermore, even if only one channel were selected, more than one receiver would provide both mission flexibility and redundancy, which are of major importance to such a mission. In addition to the receivers, the lander will provide penetrator memory and telemetered data storage for relay to Earth. Commanding up to four separate penetrators will require a carefully programmed operational sequence, but a single command frequency could be used by giving each penetrator a unique command address.

Areas Requiring Further Investigation

There are several concerns that remain to be investigated for the penetrator-beacon mission. The first, and probably foremost, is that the memory, communications, and other electrical systems must be able to function normally after the impact. Although the penetrator used in this study has a very high deceleration, it is not as high as the loads currently experienced by imaging artillery shells. The Army is developing a camera system, the Video Imaging Projectile (VIP), that can be accelerated at 16,000 Earth g when fired from a cannon.[17] The VIP is a 155-mm shell and takes images of the terrain below through a 2-in. plastic window during its trajectory, which is very similar to the proposed mission of the penetrators. Leaving the barrel at 823 m/s, the VIP spins up to 200 times a second during its 24-km flight. Its imaging camera is an electrical device that translates what it sees into one of 256 shades of gray and broadcasts its view to a ground-based computer screen below in a real-time mode. There have been two successful demonstrations of the VIP to date, and testing is expected to continue.

The orbit of the lander, which is to relay the penetrator images back to Earth, will need careful investigation and planning. The geometry of the orbit will have a major influence on the rate at which the lander can receive the penetrator-transmitted images. This has a direct influence on the lifetime requirement for the penetrators' power system. The lander's orbit will also influence the deorbit trajectory geometry of the penetrator, influencing in turn the lighting angles during imaging and the entry flight-path angle. It should be noted that the placement of penetrators deployed from approach is mostly independent of the final lander (penetrator cluster) orbit, and is governed largely by the approach geometry, i.e., the arrival velocity V^{∞} of the lander, including the declination of the arrival asymptote, as well as the entry flight-path angle.

Other areas requiring study are 1) using a hardened transparent medium that can retain most of its shape (2.4 length-to-diameter ratio) during impact for proper ground penetration, and 2) the amount of time and power required for total penetrator-to-lander data transmission vs the lander orbit. This will directly influence mass, power, and volume estimates of the penetrator system design.

Conclusions

There are many benefits that could be derived from the placement of a set of penetrator beacons in the vicinity of a landing site. The most important benefit would be in a low-cost precision-landing navigation method that meets the stringent navigation requirements of future missions. The employment of penetrators will provide the ability to perform a precision landing for little cost and minimal technical development. Because the penetrators will provide high-resolution imagery of the landing site, the landing vehicle would not be required to have a complex hazard detection and avoidance system, simplifying the system design and improving the chance of mission success. The placement of one to four radio navigation beacons would be used by a landing vehicle for precision navigation to a preselected landing site near the penetrators. The penetrators would also provide low- and high-resolution imagery of the proposed landing site and its surrounding area. These data would be invaluable to mission planners for the selection of suitable landing sites and in generating detailed surface maps that could be used in designing the traverse paths for roving vehicles and manned exploration. Another benefit from the penetrators is that they would have flown a trajectory very similar to that of a subsequent landing craft, thus improving knowledge of the local atmosphere. This improvement would assist in designing the approach trajectory to land precisely on the targeted site. The beacons on the penetrators could also be used for local rover navigation at later time. Hardware could provide direction-finding capability to allow a rover to be located with respect to the penetrator.[18] Finally, the combination of penetrators and a Mars lander is completely self-contained; there is no reliance on any other vehicle or system. The implementation of the penetrators present several design challenges, but none are insurmountable, and the overall improvement in the likelihood of mission success cannot be ignored.

Acknowledgment

The author gratefully acknowledges that the State of Texas supported this research under the Advanced Technology Program, Grant 003656089.

References

[1]Gamble, J., "JSC Pre-phase A Study, Mars Rover Sample Return Mission, Aerocapture, Entry and Landing," NASA CR-23230, May, 1989.

[2]Draper, R. F., "The Mariner Mars 11 Program," AIAA Paper 88-0067, Jan. 1988.

[3]Bourke, R. D., Kwok, J. H., and Friedlander, A., "Mars Rover Sample Return Mission," AIAA Paper 89-0417, Jan. 1989.

[4]Carter, P. H., and Smith, R. S., "Mars Rover Sample Return Lander Performance," AIAA Paper 89-0633, Jan. 1989.

[5]Pivirotto, D. S., Penn, T. J., and Dias, W. C., "Mars Rover 1988 Concepts," AIAA Paper 89-0419, Jan. 1989.

[6]Wang, T. C., Duxbury, T. C., and Synnott, S. P., "Approach for Targeting Landers and Penetrators Using Orbital Optical Navigation," American Astronomical Society, Paper 89-0404, Aug. 1989.

[7]Tuckness, D. G., " Precision Landing on Mars Using Imaging Penetrator Beacons," *Journal of Spacecraft and Rockets*, Vol. 29, No. 6, 1993, pp.

[8]Manning, L. A., "Mars Surface Penetrator System Description," NASA TM-73243, Nov. 1977.

[9]Swenson, B. L., McKay, C. P., and Carle, G. C., "A Preliminary Study of a Mars Penetrator System for Subsurface Exobiological Exploration," International Astronautical Federation, Paper 87-434, 1987.

[10]Euler, E. A., O'Neil, W. J., Rudd, R. P., Farless, C. E., Hildebrand, R. T., Mitchell, K. H., and Rourke, K. H., "Viking Navigation," Jet Propulsion Lab., Publication 78-38, Nov. 1979.

[11]French, J. R., "Mars Sample Return Mission," American Astronomical Society, Paper 86-168, July 1986.

[12]Cooley, C. G., and Lewis, J. G., "Viking Landing System Primary Mission Performance Report," NASA CR-145148, April 1977.

[13]Whitlock, C. H., and Bendura, R. J., "Inflation and Performance of Three Parachute Configurations from Supersonic Flight Test in a Low Density Environment," NASA TN-D-5296, July 1969.

[14]Young, C. W., "Empirical Equations for Predicting Penetration Performance in Layered Earth Materials for Complex Penetrator Configurations," Sandia Labs., Report SC-DR-72-0523, Albuquerque, NM, June 1972.

[15]Kaplan, D., "Environment of Mars," NASA TM-100470, Oct. 1988.

[16]Mizutani, H., and Kawashima, N., "Japanese Explorer Missions to The Moon and Venus in the Mid-1990's," *Advances in Astronomical Sciences*, Vol. 4, No. 3, 1989, pp. 242–266.

[17]Thompson, M., "Exploding Camera Relays Shots from Artillery Shell," Houston *Chronicle*, May 11, 1990, Section A, pp. 7.

[18]Costello, T., Hector, G., Rodriguez, R., and Soderland, C., "Lunar/Mars Planet Surface TNIM Final Report," NASA-JSC, IZ2/Exploration Planet Surface and Human Systems Office, Nov. 1989.